P4.11

GRAVITY WAVE-LIKE STRUCTURES OBSERVED IN ONSHORE TYPHOON BOUNDARY LAYER OF TYPHOON KIROGI (2000)

Kenichi Kusunoki [1]*
[1] Meteorological Research Institute, Japan
Kazunori Irie [2]
[2] Narita Aviation Weather Service Center, Narita, Japan

1. INTRODUCTION

Understanding the typhoon boundary layer (TBL) over land is one of the most important topics in typhoon studies as it directly affects society. In this study, an analysis of gravity wave-like structures in TBL was performed. The gravity wave-like structures were observed in the onshore outer rainband region between 320km and 450km from the typhoon center. It is at greater distances from the devastating "core" region and the typhoon circulation is relatively weak, however, low-level wind shear generated by gravity waves can be hazardous for aircraft during the takeoff and landing phases of flight (see section 2). In this study, the data from the Doppler radar for Airport Weather (DRAW), as well as aircraft soundings of wind and temperature (ACARS), provided unique data set that would permit analysis of small-scale structures embedded within the TBL and TBL environmental conditions.

2. BRIEF REVIEW OF RADAR OBSERVATIONS OF LOW-LEVEL GRAVITY WAVES

The coherent gravity wave patterns with significant horizontal wind shear have often been observed in near surface regions far away from the suggested source areas. On April 12, 1996, a commercial aircraft experienced a strong wind shear as it was departing from the Dallas-Fort Worth Airport. By using the TDWR (Terminal Doppler Weather Radar) data at the time of the incident, Meuse et al. (1996) suggested that the aircraft encountered gravity waves of 5.4km wavelength. Miller et al. (1997) examined TDWR data of Dallas-Fort Worth and Memphis airports from 1994-1997 and found eleven gravity wave-like patterns of which the wavelengths were between 2.8-11.5km. More recently, Miller (1999) reported 57 cases of gravity wave formation within the terminal areas of Dallas-Fort Worth, Memphis, and Orlando airports from 1994-1998. In Japan, Kusunoki (2005) used the Narita DRAW data and analyzed gravity waves associated with coastal cyclones and a stationary front. All the events occurred with a wind shear greater than the warning threshold commonly accepted in aviation safety.

3. STORM HISTORY (Fig. 1)

A tropical storm Kirogi began forming in the Philippine Sea on 0600UTC 3 July 2000 and strengthened into a typhoon late on 3 July. Kirogi moved north-northeast across the Hachijo and Miyake Islands and its center passed near the eastern coast of the Boso Peninsula on 8 July. Kirogi continued to move north-northeastward and became an extratropical cyclone late on 8 July near the eastern coast of Hokkaido Island.

Gravity wave-like structures were observed at around 2140 Japan standard time (JST) 7 July - 0000 JST 8 July 2000 with the Narita DRAW. Geostationary Meteorological Satellite (GMS) imagery at 2239 JST indicated an extensive cloud system over the Kanto Plain associated the Kirogi outer rainband region (Fig. 3).

Corresponding author address:
* Kenichi Kusunoki, Meteorological Research Institute, 1-1,Nagamine, Tsukuba, Japan
E-mail: kkusunok@mri-jma.go.jp

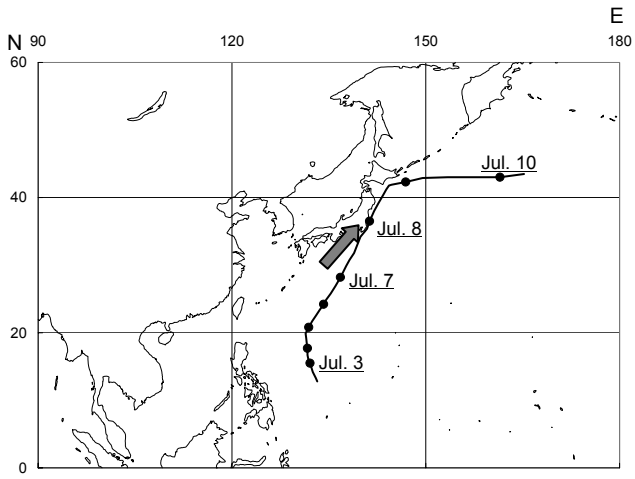

FIG. 1. Best track of Typhoon Kirogi between 2 July and 10 July 2000. The arrow shows the study area.

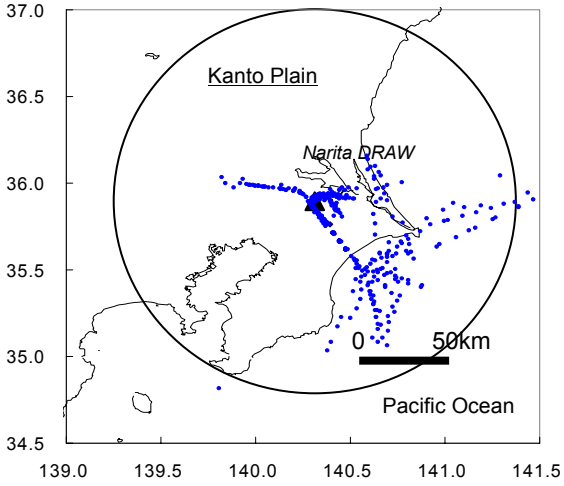

Fig. 2. Map showing the study area. The triangle indicates the position of the Narita DRAW. The shorelines are outlined by the solid lines. Dots indicate the positions of ACARS data around Narita International Airport from the surface to 3 km AGL.

3. DATA

The data used in this study include (a) the Narita DRAW data and (b) the ACARS data from the surface to a 3000-m height around Narita International Airport. The locations where the data were taken are shown in Fig. 2. In addition to the above data, geostationary satellite data, surface pressure and wind data at Narita International Airport, and surface temperature data from the Automated Meteorological Data Acquisition System (AMeDAS) were also used.

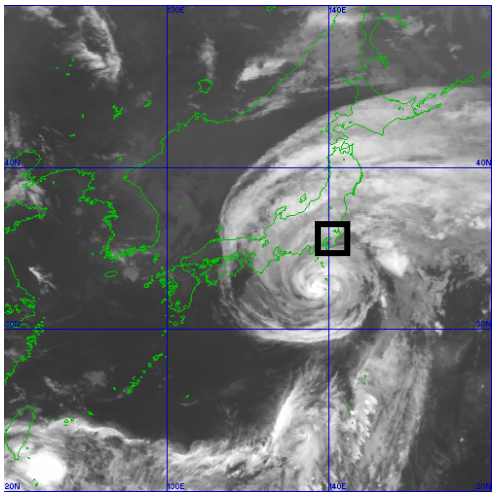

FIG. 3. GMS satellite infrared image at 2239 JST 7 Jul 2000. The rectangular window covers the study area.

a. The Narita DRAW

The Data from Doppler Radar for Airport Weather (DRAW) of at Narita International Airport observed gravity wave-like structures. The DRAW velocity dealiasing algorithm (Kusunoki et al. 1997) correctly dealiases velocities even in a complicated circulation associated with the gravity wave.

b. ACARS

Many commercial aircraft report wind and temperature data automatically, a system that is referred to as ACARS data. Because aircraft near Narita international airport transmitted ACARS data around the study period, the data are used to obtain wind and temperature profiles in order to determine the environmental conditions of the gravity waves.

4. RESULTS

a. Characteristics of the internal gravity waves

Gravity wave-like structures were observed at around 2140 JST 7 July - 0000 JST 8 July with the Narita DRAW. For the first 30min, the horizontal wavelength was around 7.0-10.0 km but the direction of

propagation was unclear. Then waves of wavelength of 4.0km became the dominant feature and persisted for about 2 hours. The complicated change of the wave patterns reveals the complex environment of onshore rainbands examined in this study. In this study, we will focus on the 4km-wavelength wave. Figure 4 shows the distribution of radial convergence from the PPI scan of the Doppler velocity near the surface (the lowest elevation is 0.8º) of the Narita DRAW at 2310 JST. The convergence patterns showed that the wave region spread over 80 km horizontally. Note that the radial convergences (i.e., the low-level wind shears) associated with the wave patterns are greater than the warning threshold commonly accepted in aviation safety (2.5 $ms^{-1}km^{-1}$: Wilson et al. 1984). The wave packet moved northward mainly following the direction of Kirogi movement, while the direction of wave propagation was toward 45º (NE), which was rotated roughly 180º counterclockwise from the ambient wind vectors at the surface. Differently from hurricane boundary layer rolls, which are almost aligned with the mean wind direction, the orientation of the streaks in this case was nearly perpendicular to it. The ground-relative phase speed of the waves varied from roughly 0.0 to 5.0 m s^{-1}. Upstream of the gravity waves, a strong convective cell embedded in stratiform outer rainband was observed (not shown). The observation strongly suggests that the cell was the source of the wave disturbance.

b. The environmental conditions

Figures 5a and 5b show the averaged wind hodograph and the averaged vertical profile of wave-parallel wind speed between 1900-2200 JST. These data are obtained from ACARS soundings. According to the wind hodograph, the wind direction veered significantly from northwesterly near the surface to southeasterly at 3000 m AGL. The maximum wind speed was 19.0 ms^{-1} at 1000 m AGL. The ground-relative phase speed and the direction of propagation of the waves are marked in Fig. 5a. The wind direction of the mean (lower) region is the opposite direction to the wave propagation.

The Brunt–Väisälä frequency (BVF) derived from the averaged temperature profile between 1900-2200 JST, also obtained from the ACARS soundings, is indicated in Fig. 5c. BVF was 1.5 x 10^{-2} s^{-1} at 600 m AGL, associated with the low-level northeasterly wind. The low-level northeasterly flow with relatively cold air can also be seen in the surface wind field (Fig. 6). The low-level cold northeasterly flow and the warm southeasterly flow from the Kirogi contributed to the formation of the stable layer with significant vertical wind shear.

The square of the Scorer parameter *l* is calculated from the profiles of the temperature and wind of ACARS (Fig. 5d).

$$l^2 \equiv \frac{N^2}{(\bar{u}-c)^2} - \frac{d^2\bar{u}/dz^2}{\bar{u}-c}$$

where is the Brunt-Väisälä frequency, $\bar{u}$is the component of the ambient flow normal to the waves, and *c* is the horizontal phase speed. Near the surface, l^2 decreased with height and became less than the horizontal wavenumber k^2 near 600 m AGL. This shows the existence of a layer at a depth of about 600 m in which the waves are trapped. In order to assess the relative contributions of static stability and wind profiles to l^2, each of the two terms are also shown in Fig. 5d. It is indicated that the wind curvature is more prevalent than the stability for trapping wave energy.

c. Surface pressure perturbation

Several investigators have reported surface pressure perturbations affected by the passage of waves as one of the characteristics of internal gravity waves (e.g., Kusunoki and Eito 2003). We examine the relationships between the surface pressure perturbations and surface wind speed perturbations associated with the waves. Figure 7 shows the surface pressure traces and the surface wind speed traces observed at the Narita Airport. To isolate the oscillations due to the gravity waves from the raw data, a 10-min running average has been applied to the pressure data and then, the means and trends were removed. The amplitude is about 0.5-1.0 hPa for the pressure perturbations and about 5.0-7.0 ms^{-1} for the wind speed perturbations. The perturbation

period of about 20 minutes in the Narita Airport suggests reflecting the passages of the wave of wavelength 4.0 km and with phase speed of about 3.3 ms^{-1}. Vertical dashed lines of the constant phase are drawn for every 90º. The trough (ridge) of the surface perturbation pressure is roughly a 180º phase shift from the trough (ridge) of the surface wind speed. The phase relationship between the horizontal velocity and the perturbation pressure is consistent with that of the internal gravity waves.

5. DISCUSSION AND CONCLUSIONS

In this study, an observational analysis of the TBL in the onshore outer rainband region of Typhoon Kirogi (2000) on 7 July 2000 was performed. High-resolution observations obtained with the DRAW revealed the existence of long-lived, kilometer-scale, coherent streaks within the TBL were dominated. The horizontal wavelength was approximately 7-10 km (ground-relative phase speed: unclear) for the first 30 min, then changed 4 km (ground-relative phase speed: 0.0 to 5.0 m s^{-1}) and persisted for over 2 hours. The wave packet moved northward mainly following the direction of Kirogi movement, while the direction of wave propagation was rotated roughly 180º counterclockwise from the ambient wind vectors at the surface. Differently from hurricane boundary layer rolls, which are almost aligned with the mean wind direction, the orientation of the streaks in this case was nearly perpendicular to it. It is noteworthy that the streaks occurred with a horizontal wind shear greater than the warning threshold (i.e., 2.5 $ms^{-1}km^{-1}$) commonly accepted in aviation safety. The profiles from ACARS revealed two distinct air masses, and the wind direction veered significantly throughout the 3 km. One was the cold northeasterly flow below 600 m AGL and the other was associated with the southeasterly flow in the hurricane circulation over the Pacific Ocean. It is suggested that the high stability below 600 m AGL, combined with negative values of the wind curvature term that associated with the flow that opposed the wave motion, created large values of the Scorer parameter and assisted in wave propagation. The frequency and the phase of surface pressure perturbations are consistent with theoretical relations with gravity waves, suggesting that they were caused by the passage of the gravity waves. These results indicate that the TBL acts as a duct and the gravity waves were trapped vertically and reflected downward.

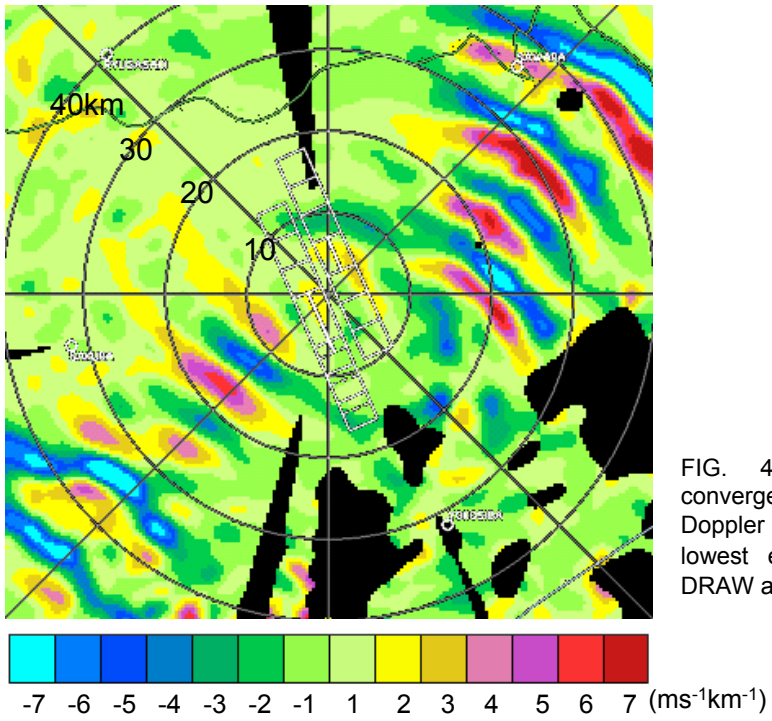

FIG. 4. The distribution of radial convergence from the PPI scan of the Doppler velocity near the surface (the lowest elevation is 0.8º) of the Narita DRAW at 2310 JST.

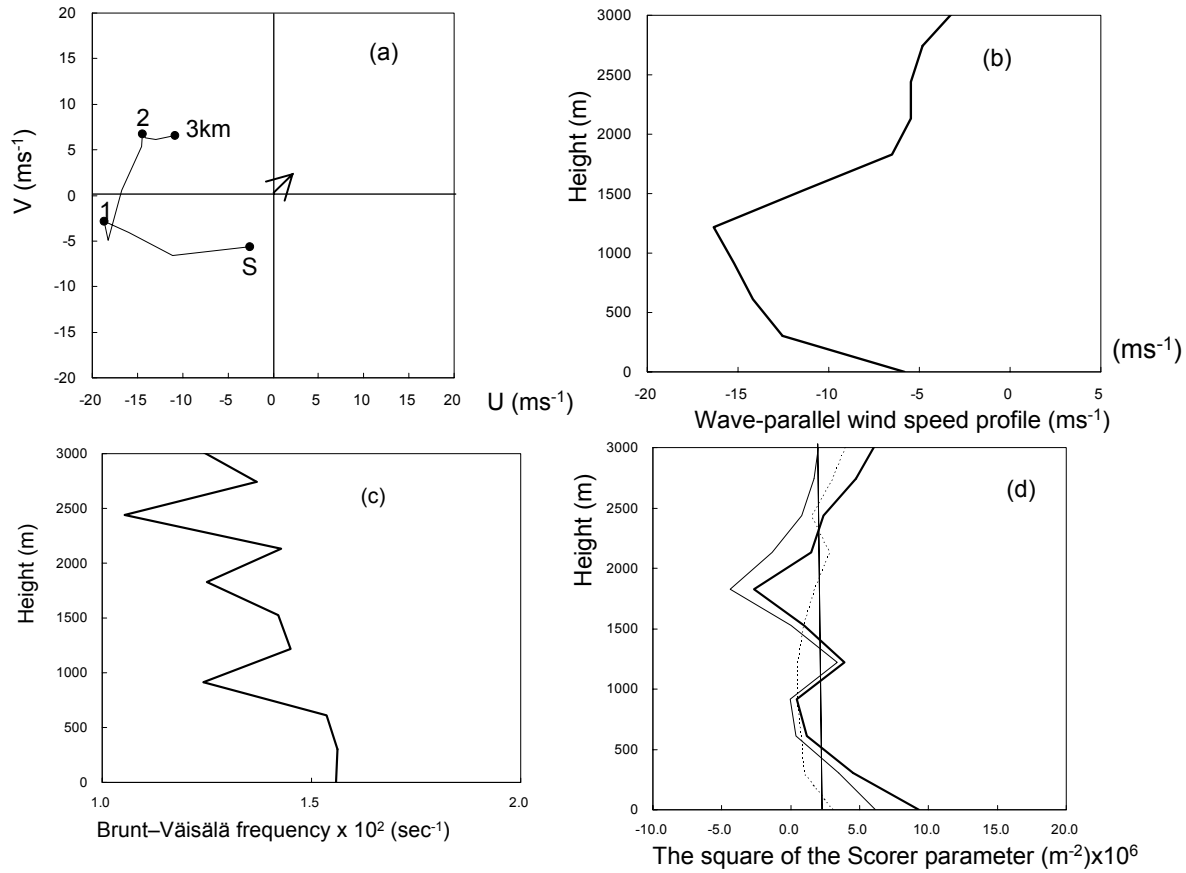

FIG. 5. The averaged vertical profiles calculated from temperature and wind of ACARS data on 7 July 2000: (a) Wind hodograph. The ground-relative phase speed and the direction of propagation of the waves are marked with the arrow. (b) Wave-parallel wind speed profile. (c) Brunt–Väisälä frequency. (d) The square of the Scorer parameter (bold), the static stability term (thin, solid), and the wind curvature term (dashed). The vertical line indicates the square of the horizontal wave number of the observed wave.

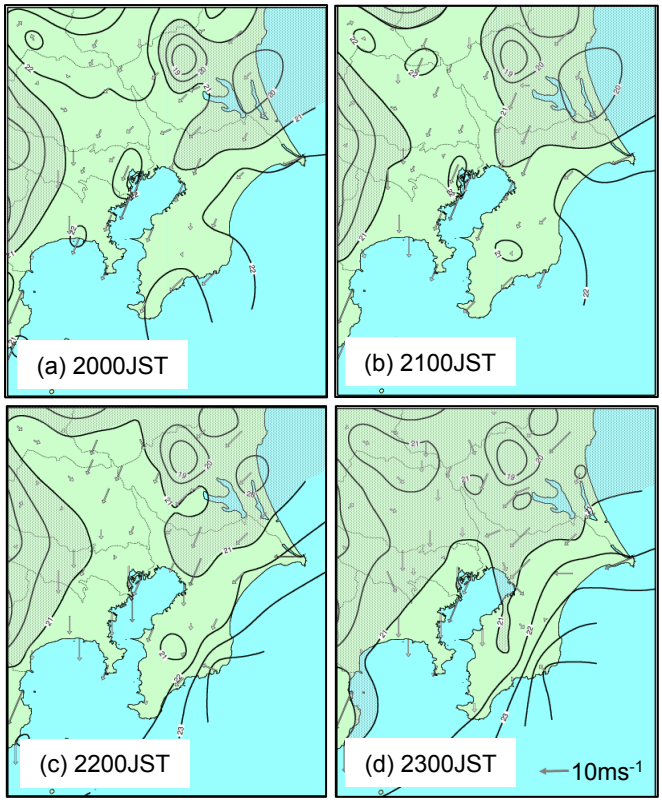

FIG. 6. Time series of surface temperature and wind fields from the AMeDAS surface stations. Wind speed scale (10 m s^{-1}) is indicated. Surface temperature is contoured every 2 °C with shading below 21°C.

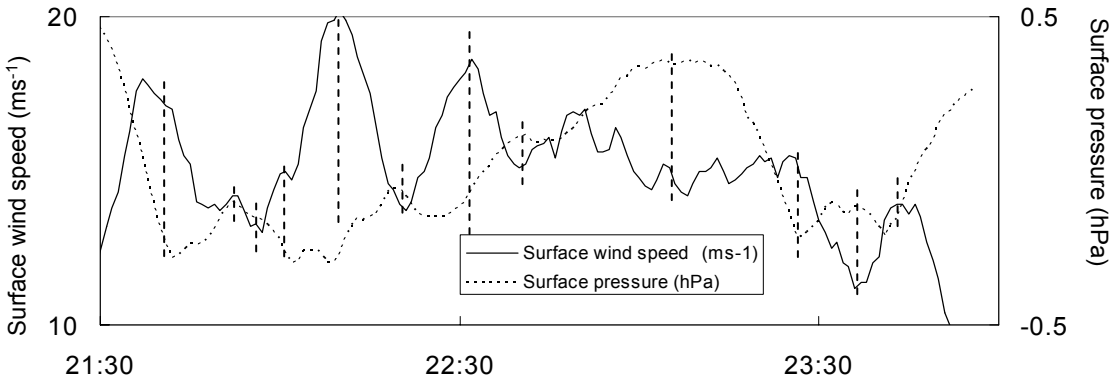

FIG. 7. Surface pressures and surface wind speeds at the Narita Airport. Vertical dashed lines indicate the times at which inverse correlation can be clearly seen.

REFERENCES

Kusunoki, K., 2006: A climatological study of low-level internal gravity waves in precipitating environments over the Kanto plain, Japan. *12th Conf. on Aviation Range and Aerospace Meteorology*, Amer. Meteor. Soc., P5.7.

Kusunoki, K. and H. Eito., 2003: Analytical studies of low-level internal gravity waves over the Kanto Plain associated with a stationary front. *Mon. Wea. Rev*., 131, 236-248.

Kusunoki, K. O. Suzuki, and H. Ohno., 1997: Hybrid Algorithm for Doppler Velocity Dealiasing with Dual PRF Data. Preprints, *7th Conf. on Aviation, Range, and Aerospace Meteorology*, Amer. Meteor. Soc., 346-349.

Meuse, C., M. Isaminger, M. Moore, D. Rhoda, F. Robasky, M. Wolfson, 1996: Analysis of the 12 April 1996 wind shear incident at DFW Airport. *Preprints of Workshop on Wind Shear and Wind Shear Alert Systems*, Amer. Meteor. Soc., 23-33.

Miller, D. W., B. G. Boorman, R. F. Ferris, and T. M. Rot, 1997: Characteristics of thunderstorm induced gravity waves using Doppler radar and tower instrumentation. *Preprinted, 28th Conf. on Radar Meteorology,* Amer. Meteor. Soc., 165-167.

Miller, D.W., 1999: Thunderstorm induced gravity waves as a potential hazard to commercial aircraft. *Preprinted, 8th Conf. on Aviation, Range and Aerospace Meteorology*, Amer. Meteor. Soc., 225-229.

Scorer, R., 1949: Theory of waves in the lee of mountains. *Quart. J. Roy. Meteor. Soc.,* **75,** 41–56.

Wilson, J. W., R. D. Roberts, C. Kessinger, and J. McCarthy, 1984: Microburst wind structure and evaluation of Doppler radar for airport wind shear detection. *J. Climate Appl. Meteor.*, **23**, 898-915.